The Role of Charge States in the Atomic Structure of Cu n and Pt n (n = 2−14 atoms) Clusters: A DFT Investigation

ARTICLE *in* THE JOURNAL OF PHYSICAL CHEMISTRY A · OCTOBER 2014

Impact Factor: 2.69 · DOI: 10.1021/jp508220h · Source: PubMed

5 AUTHORS, INCLUDING:

Anderson Silva Chaves
University of São Paulo
8 PUBLICATIONS **8** CITATIONS
SEE PROFILE

Gustavo G. Rondina
Technical University Darmstadt
3 PUBLICATIONS **18** CITATIONS
SEE PROFILE

P. L. Tereshchuk
University of São Paulo
24 PUBLICATIONS **83** CITATIONS
SEE PROFILE

THE JOURNAL OF PHYSICAL CHEMISTRY A

Article

pubs.acs.org/JPCA

The Role of Charge States in the Atomic Structure of Cu_n and Pt_n (n = 2−14 atoms) Clusters: A DFT Investigation

Anderson S. Chaves,*[,†] Gustavo G. Rondina,*[,†] Maurício J. Piotrowski,*[,§] Polina Tereshchuk,*[,‡] and Juarez L. F. Da Silva*[,‡]

[†]São Carlos Institute of Physics, and [‡]São Carlos Institute of Chemistry, University of São Paulo, 13560-970 São Carlos, São Paulo, Brazil

[§]Departamento de Física, Universidade Federal de Pelotas, Caixa Postal 354, 96010-900 Pelotas, Rio Grande do Sul, Brazil

Supporting Information

ABSTRACT: In general, because of the high computational demand, most theoretical studies addressing cationic and anionic clusters assume structural relaxation from the ground state neutral geometries. Such approach has its limits as some clusters could undergo a drastic structural deformation upon gaining or losing one electron. By engaging symmetry-unrestricted density functional calculations with an extensive search among various structures for each size and state of charge, we addressed the investigation of the technologically relevant Cu_n and Pt_n clusters for n = 2−14 atoms in the cationic, neutral, and anionic states to analyze the behavior of the structural, electronic, and energetic properties as a function of size and charge state. Moreover, we considered potentially high-energy isomers allowing foresight comparison with experimental results. Considering fixed cluster sizes, we found that distinct charge states lead to different structural geometries, revealing a clear tendency of decreasing average coordination as the electron density is increased. This behavior prompts significant changes in all considered properties, namely, energy gaps between occupied and unoccupied states, magnetic moment, detachment energy, ionization potential, center of gravity and "bandwidth" of occupied d-states, stability function, binding energy, electric dipole moment and sd hybridization. Furthermore, we identified a strong correlation between magic Pt clusters with peaks in sd hybridization index, allowing us to conclude that sd hybridization is one of the mechanisms for stabilization for Pt_n clusters. Our results form a well-established basis upon which a deeper understanding of the stability and reactivity of metal clusters can be built, as well as the possibility to tune and exploit cluster properties as a function of size and charge.

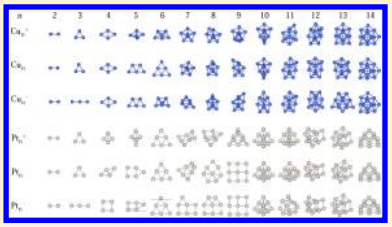

I. INTRODUCTION

It has been known that chemical and physical properties of subnanometer clusters can exhibit a strong dependence on their number of atoms.[1,2] To further investigate this matter, several theoretical approaches have been employed to address the size evolution of such clusters and, in particular, of neutral systems.[3,4] However, even though most of the theoretical studies tend to focus on neutral clusters,[4,5] the majority of the experimental research in this field has concentrated on cationic and anionic systems[6−9] due to experimental difficulties to prepare neutral clusters in a laboratory. For instance, ion-mobility spectrometry reveals that the addition (release) of one electron to (from) a cluster can produce pronounced changes in its geometry, hence, affecting its chemical and physical properties, as can be illustrated by the case of Au clusters.[7] Therefore, the need to bridge the gap between theory and experiments brings forth a great interest in understanding the role of charge states in the properties of charged clusters from a theoretical standpoint, in particular, in small and medium-sized transition-metal (TM) charged clusters, given the wide range of applications of TM systems.[10−14]

Toward a deeper comprehension of the role of charge states, the determination of the atomic structure of cationic (+), neutral (0), and anionic (−) TM clusters is a key requisite, which can be fulfilled by global or local optimization algorithms. For example, several global optimization algorithms have been proposed to explore the potential energy surface (PES), such as the Basin Hopping Monte Carlo (BHMC),[15,16] the Revised BHMC (RBHMC),[17] Genetic Algorithms,[18] and Dynamic Lattice Searching.[19] Furthermore, local optimization algorithms have been widely employed,[3−5,20] notably for small clusters as their PESs are less intricate than those of systems with a larger number of atoms, given that there is a strong assumption that the number of local minima and transition states of a PES scales exponentially with the number of atoms.[21,22]

The investigation of the putative global minimum for different charge states is computationally expensive due to the number of charge states for each system (e.g., cationic, neutral, and anionic), and hence, from our knowledge, most of the studies for cationic and anionic clusters are based on the local optimization of a single atomic configuration, namely, the neutral lowest energy configuration.[23,24] Thus, it is a good approximation only for the cases in which the addition or

Received: August 13, 2014
Revised: October 19, 2014

   dx.doi.org/10.1021/jp508220h | J. Phys. Chem. A XXXX, XXX, XXX−XXX

release of one electron does not induce a large atomic distortion of the clusters; however, experimental evidence has indicated that it might not be the case for every system.[7,8,14,25,26]

In this paper, we address the charge effects in TM clusters by determining charged cluster structures via symmetry-unrestricted structural optimizations using density functional theory (DFT) calculations through an extensive search among various geometries for different charge states. Although this procedure is much more computationally expensive than simply relaxing the neutral geometries after adding or removing an electron, it provides a more thorough exploration of the PES, increasing the chances of yielding low-energy isomers. In this investigation we selected two model systems of great importance in the field of TM clusters,[7,27−32] which are Cu_n (3d states) and Pt_n (5d states) clusters with sizes ranging from n = 2 to 14 atoms. These two systems have different chemical and physical properties due to the occupation of the d states, differences in the localization of the 3d and 5d states, and total number of electrons, and, hence, they provide an ideal ground to study charge state effects in TM clusters.

II. THEORETICAL APPROACH AND COMPUTATIONAL DETAILS

Total Energy Calculations. Our calculations are based on spin-polarized DFT within the generalized gradient approximation[33] proposed by Perdew−Burke−Ernzerhof (PBE).[34] To solve the Kohn−Sham (KS) equations, we employed the all-electron full-potential Fritz-Haber Institute Ab Initio Molecular Simulations (FHI-aims) package[35,36] in which the electrons are described by the scalar-relativistic framework within the zeroth-order approximation.[37] The KS orbitals are expanded in numerical atom-centered orbitals (NAOs),[38,39] which were hierarchically constructed from the minimal basis to meV-level total energy convergence.[35]

Seeking to minimize the computational cost, our calculations were performed using two steps: (i) Relaxation of the atomic configurations using a smaller NAOs basis (i.e., light-tier1 according to FHI-aims terminology), which is the first improvement from the minimal basis by adding further radial functions with an overall cutoff radius of 5.0 Å. A broadening parameter of 0.10 Å was used for the smearing of the electronic states, while the total energy convergence was set up to 10^{-4} eV, and the equilibrium configuration was found once the atomic forces are smaller than 0.10 eV/Å. (ii) A final optimization was performed using a larger basis set, namely, light-tier2, and using an overall cutoff radius of 6.0 Å, a broadening parameter of 0.01 eV, a total energy convergence of 10^{-5} eV, and the equilibrium configuration is reached once the atomic forces are smaller than 0.010 eV/Å on all atoms.

Atomic Configurations. We employed a set of structural design principles to obtain a reliable set of atomic configurations for Cu_n and Pt_n (n = 2−14) in the cationic (TM_n^+), neutral (TM_n^0), and anionic (TM_n^-) states. Our strategy is based on the following steps: (i) An initial set of different configurations was generated for Cu_n^0 and Pt_n^0 using results from the literature.[4,5] (ii) This set of structures was incremented by configurations obtained from our Revised Basin Hopping Monte Carlo (RBHMC) implementation[17] within Sutton-Chen empirical potentials[40] and designed structures using the Avogadro package.[41] (iii) All neutral configurations were optimized using the Broyden−Fletcher−Goldfarb−Shanno (BFGS) algorithm with trusted region[35] as implemented in FHI-aims. (iv) Structural crossover among the lowest energy configurations obtained for Cu_n^0 and Pt_n^0 from the aforementioned set was performed. For example, the lowest energy configuration identified for Pt_{10}^0 was used as input for Cu_{10}^0, and vice versa. (v) In case that two initial configurations yielded nearly the same local minimum configuration, one of the configurations was replaced by a new configuration. (vi) Once a set of local minimum configurations in the neutral state was obtained (e.g., 4n, n = number of atoms in the cluster), the whole set of configurations was reoptimized in the cationic and anionic states.

Analyses. To obtain a deep understanding of the role of charge states in the physical and chemical properties of Cu_n and Pt_n clusters as a function of size, we performed several analyses. We calculated the average effective coordination number, ECN, and average weighted bond lengths, d_{av}, using the effective coordination concept,[42−44] and we found the atomic radius of the clusters by measuring the distance between the farthest atom and the geometric center of the cluster. To understand the energetic stability, we calculated the binding energies per atom, E_b,[45] and the stability function, ΔE^2, which yields the relative stability of a particular cluster, TM_n, with respect to its neighboring sizes, TM_{n-1} and TM_{n+1}.[45,46] Thus, E_b and ΔE^2 for the cationic, neutral, and anionic states were calculated using the following equations:

$$E_b^{TM_n^+} = (E_{tot}^{TM_n^+} - (n-1)E_{tot}^{TM_1^0} - E_{tot}^{TM_1^+})/n \quad (1)$$

$$E_b^{TM_n^0} = (E_{tot}^{TM_n^0} - nE_{tot}^{TM_1^0})/n \quad (2)$$

$$E_b^{TM_n^-} = (E_{tot}^{TM_n^-} - (n-1)E_{tot}^{TM_1^0} - E_{tot}^{TM_1^-})/n \quad (3)$$

$$\Delta E_n^2 = E_{tot}^{TM_{n-1}} + E_{tot}^{TM_{n+1}} - 2E_{tot}^{TM_n} \quad (4)$$

where $E_{tot}^{TM_n^{+/0/-}}$ and $E_{tot}^{TM_1^{+/0/-}}$ are the total energies of the TM_n clusters and free atoms, respectively, in the cationic, neutral, and anionic charge states. The equation for ΔE^2 can be applied for the three charge states.

For the electronic properties, we calculated the detachment energy, DE (DE = $E_{tot}^{TM_n^0} - E_{tot}^{TM_n^-}$ and the ionization potential, IP (IP = $E_{tot}^{TM_n^+} - E_{tot}^{TM_n^0}$). For calculations without relaxations of the TM_n^+ and TM_n^- clusters, namely, using the same lowest energy TM_n^0 configuration for all charge states, DE and IP are called vertical DE (vDE) and vertical IP (vIP). For the case in which relaxation effects are taken into account both quantities are called adiabatic DE (aDE) and adiabatic IP (aIP). The relaxation effects can be taken into account by using local optimization techniques, which relaxes the structure to one of the nearest local minimum configurations, however, an increase or decrease in the number of electrons can change the configuration into a complete different structure. For such cases, performing global optimization[17] is a better suited as a relaxation technique, nevertheless it is also possible to consider a large number of structures in order to identify the lowest energy configuration for a particular cluster and charge state. As discussed above, the latter approach is employed in this work.

The hybridization between the delocalized s states and the localized d states leads to the metallo-covalent binding contribution, which affects the binding energy, in particular, for heavy systems.[47] The sd hybridization can be accessed by the hybridization index as defined by Häkkinen,[47] in which the sd hybridization is defined for a N atom cluster as

dx.doi.org/10.1021/jp508220h | J. Phys. Chem. A XXXX, XXX, XXX−XXX

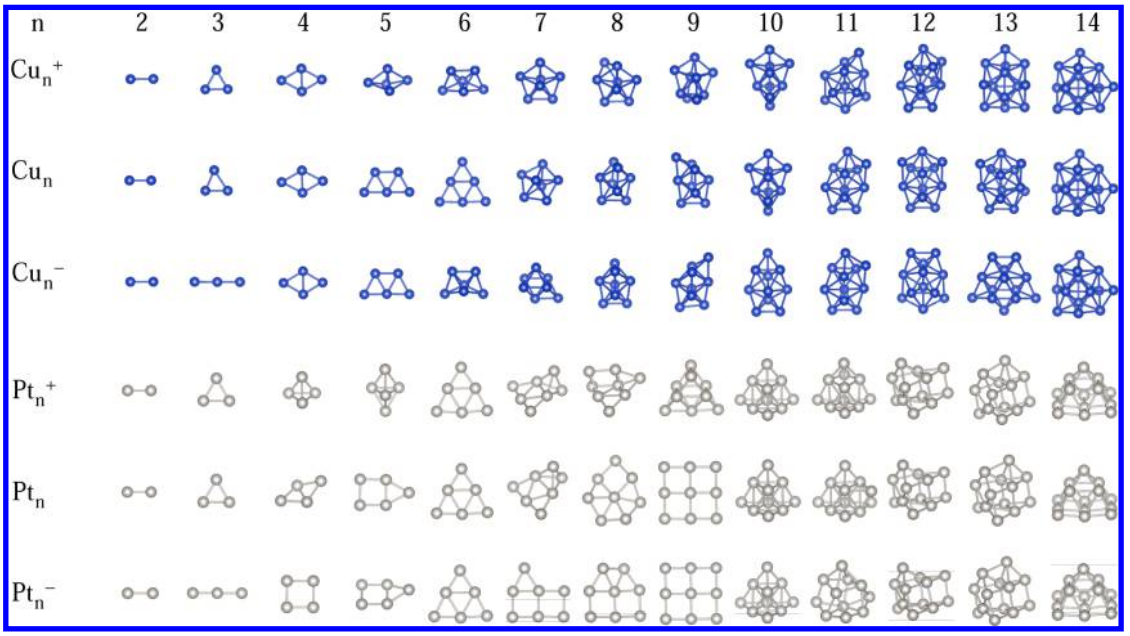

Figure 1. Putative global minimum DFT-PBE configurations for the Cu_n and Pt_n (n = 2−14) clusters in the cationic, neutral, and anionic states.

$$H_{sd} = \sum_{I=1}^{N} \sum_{i=1}^{occ} w_{i,s}^{(I)} w_{i,d}^{(I)} \quad (5)$$

where $w_{i,s}^{(I)}$ ($w_{i,d}^{(I)}$) is the projection of KS orbital i onto the s(d) spherical harmonic centered at atom I, integrated over a sphere of specified radius. Thus, this analysis provides only a qualitative characterization of the orbital contributions to the chemical bonding.

III. RESULTS

Using the structural design principles mentioned above, we obtained the putative global minimum configurations (lowest energy structures, Figure 1) and a large number of high-energy isomers. To improve the atomistic understanding of the physical and chemical properties and highlight the role played by the charge states, we calculated several structural, energetic, and electronic properties for the putative global minimum structures (below) and for the higher energy isomers (Supporting Information).

A. Structural Properties. *Putative Global Minimum Structures.* We found that the charge state plays a crucial role in the putative global minimum configurations, which can be measured by the number of clusters with nearly the same geometry for all charge states. We found nearly the same structure only in the cases of n = 2,4,14 for Cu_n and n = 2,6,10,12,13,14 for Pt_n, while the remaining clusters have different structures, Figure 1. For example, both Cu_3^+ and Cu_3^0 have a triangular structure, while Cu_3^- has a linear structure, and the same trend occurs also for Pt_3. Pt_4 shows an interesting behavior, namely, an evolution from two-dimensional (2D) to three-dimensional (3D) configurations by decreasing the number of electrons in the cluster, i.e., from anionic (square), neutral (nearly planar rhombus), to cationic (triangular pyramid). A similar structural transition, namely, anionic (2D) to cationic (3D) can be seen also for Cu_5, Pt_5, Pt_7, Pt_8, Pt_9, which clearly indicates that a change in the number of electrons by any unit can modify the cluster geometry completely.

We found that the transition from 2D to 3D configurations is dependent on the charge state. For Cu_n, the 2D−3D transition occurs at n = 4−5 for Cu_n^+, n = 6−7 for Cu_n^0, and n = 5−6 for Cu_n^{0-}, while we found n = 3−4 for Pt_n^+, n = 6−7 for Pt_n^0 and n = 9−10 for Pt_n^-. Thus, we obtained a larger number of 2D structures for Pt_n than for Cu_n, i.e., the Pt_n clusters have an increased tendency for 2D configurations. However, it is important to mention that the first high-energy isomers for the Pt_n clusters have relative energy differences smaller than 25 meV/atom (nearly K_bT at room temperature) and often show an opposite trend (i.e., 3D instead of 2D structures and vice versa). These results highlight the practical difficulties in determining the cluster sizes that occur in the 2D−3D structure transition.

Our 3D Cu_n structures (n > 7) are based on the layered Cu_7 structure, which has a pentagonal bipyramid geometry. Our results for Cu_n are in good agreement with previous tight-binding[48] and DFT-GGA calculations.[49] In the size range of n = 10−14 atoms, Pt_n clusters display a preference for layered and pyramidal geometries, while in the cationic state the growth is slightly more complicated, presenting tetrahedral-like geometric motifs of Pt_4^+ and Pt_5^+, planar for Pt_6^+ and quasi-planar for Pt_7^+. For Pt_n, we identified new lowest energy configurations, which are different from previous studies for few systems, namely, Pt_7^0, Pt_8^0, and Pt_{12}^0.[50−55] For example, our configurations are ∼18, 19, and 5 meV/atom lower in energy than the configurations reported by Kumar.[55] Furthermore, we found a square structure for Pt_4^- instead of the rhombohedral geometry reported by Fortunelli.[56]

Effective Coordination Number, Bond Lengths, and Atomic Radius. We found a stronger dependence of the d_{av}^{Pt} parameters on the charge state, in particular for small Pt_n clusters, Figure 2, which can be related to the changes in the coordination of the clusters induced by the addition or release of one electron. For both systems, we obtained that d_{av} increases with the number of atoms in the clusters (except small down oscillations for Pt_n), which is expected as the bond lengths increase with an increasing in the coordination number.

dx.doi.org/10.1021/jp508220h | J. Phys. Chem. A XXXX, XXX, XXX−XXX

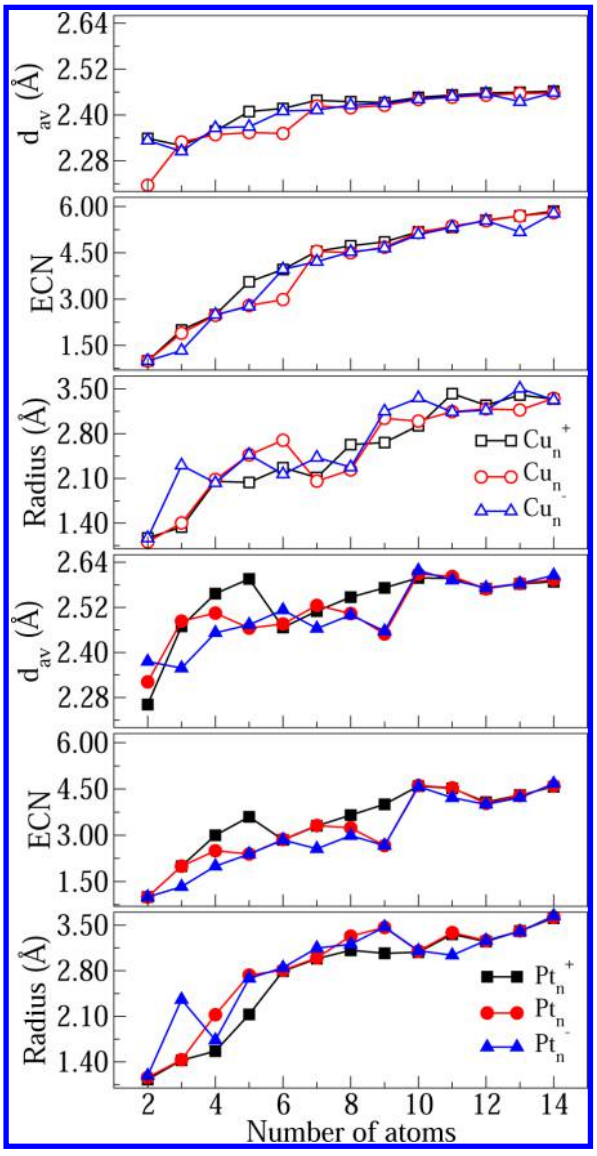

Figure 2. Average weighted bond length (d_{av}), effective coordination number (ECN), and atomic radius (Radius) of the Cu_n and Pt_n clusters in the lowest energy configurations (cationic, neutral, and anionic states) as a function of the number of atoms (n = 2−14).

Furthermore, $d_{av}^{Pt} > d_{av}^{Cu}$ for $n > 3$, which is expected due to the larger lattice constant of bulk Pt compared with bulk Cu.[57]

For $n \geq 6$ atoms, Pt clusters are less compact than Cu clusters, a general trend found in larger clusters. In the case of smaller clusters ($n < 6$), ECN^{Cu} is almost the same as ECN^{Pt} for all charge states. In particular, kinks can be observed in the ECN function, which results from the 2D to 3D transitions (e.g., at n = 4−5, n = 6−7, and n = 5−6 for Cu_n). For Pt_n, there are planar structures even for n = 9 for neutral and anionic states with a planar-to-3D turnover occurring from 9 to 10 Pt atoms. For Pt_n^+ this turnover occurs much earlier at n = 3−4 atoms. The dependence of the d_{av} and ECN as a function of the number of atoms directly determines the dependence of the atomic radius of the clusters, which show similar trends as d_{av} and ECN.

B. Energetic Properties. The energetic properties, the relative stability, and the binding energy are summarized in Figure 3. As expected for both systems, we found that the binding energy increases in absolute value almost monotonically with the size for all charge states, which is expected as at the limit of large size particles, the binding energy should reach the bulk value (i.e., the surface effects should be negligible). In agreement with previous results available for Cu_n clusters,[45,48,49,58] we found that charged clusters have larger absolute values for the binding energy than neutral clusters, while anionic clusters lie in between them. The same binding-energy behavior for the charge states is obtained for Pt_n systems.

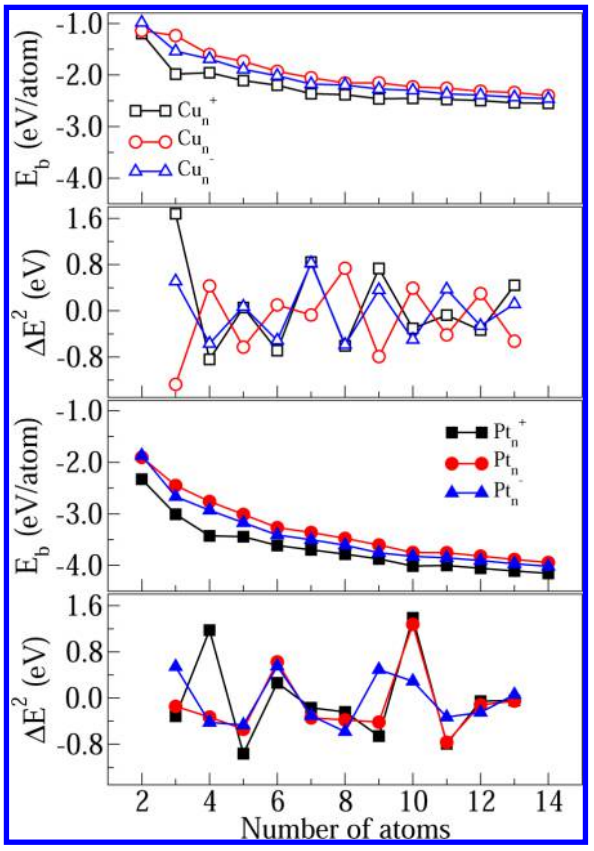

Figure 3. Binding energy, E_b, and relative energy stability, ΔE^2, for the Cu_n and Pt_n clusters in the cationic, neutral, and anionic charge states as a function of the number of atoms in the clusters.

For Cu_n, we observed an odd−even alternation effect in the relative stability as a function of cluster size for all charge states; that is, charged clusters are more stable when the n is odd, and neutral clusters are more stable when n is even. For example, Cu_8 (Cu_9^+) presents greater value for ΔE^2 than Cu_9 (Cu_{10}^+). Our stability results are in good agreement with the literature[45] and can be explained by the presence or absence of unpaired electrons of Cu clusters (electron pairing effect). This effect can be correlated with the reactivity of the clusters; for example, in the recent study of Cu_n^- (n = 7−11) clusters, it was revealed that the even-sized clusters are more reactive with O_2 than the odd-sized clusters.[59]

Regarding the E_b curves for Pt_n clusters, some discrepancies from the observation made above occurs when the curve seems to fold, such as for Pt_4^+, Pt_6^+, Pt_{10}^+, Pt_3^-, Pt_6^-, Pt_9^-, Pt_{10}^-, Pt_6^0, and Pt_{10}^0. These local maxima (humps) correspond to higher stability of these clusters, in line with results obtained from stability curve (ΔE^2) for Pt_n clusters, in which there are clear peaks appearing at the same specific sizes. Here, we note that regardless of the charge states, both Pt_6 and Pt_{10} have higher stability. As stressed above, these clusters also present the same

dx.doi.org/10.1021/jp508220h | J. Phys. Chem. A XXXX, XXX, XXX−XXX

geometric structures for all charge states. Furthermore, our results agree with Adlhart et al.[13], which suggested that Pt_4^+, Pt_{10}^+, Pt_6^-, Pt_9^-, and Pt_{10}^- are magic clusters due their low reactivity with CH_4.

C. Electronic Properties. To obtain a deep understanding of the electronic properties, we calculated the following properties: total magnetic moment m_T, electric dipole moment, energy gap between the highest occupied molecular orbital (HOMO) and the lowest unoccupied molecular orbital (LUMO) E_g, center of gravity of the occupied d states C_g, bandwidth, hybridization index for the s and d states, detachment energy (DE), and the ionization potential (IP). The results are shown in Figures 4, 5, and 6.

Total Magnetic Moment. For the Cu_n^0 clusters, m_T has a well-established oscillatory-like zigzag behavior, alternating from 0 μ_B for even number of atoms to 1 μ_B for odd number of atoms, while for Cu_n^- and Cu_n^+, we obtained an opposite trend, namely, 0 μ_B and 1 μ_B for odd and even number of atoms, respectively. This behavior can be explained by the electronic structure of the neutral Cu atom, $3d^{10}4s^1$, which shows an unpaired electron for an odd number of Cu atoms in the cluster, which gives rise to the magnetic moment. Thus, the spin polarization occurs in the delocalized s-like orbitals.[60] In contrast with Cu_n, the resulting magnetic moment in Pt_n clusters is due to the partial occupation of the 5d states[60], and the m_T results for the Pt_n clusters do not show an oscillatory behavior; hence, there is no correlation with even or odd number of valence electrons. However, it shows an interesting feature: m_T has a maximum value for n = 10, which can be favored by its symmetric pyramidal structure (not Jahn–Teller distorted) allowing high exchange coupling like Hund's rules for regular atoms. Our m_T results are in a good agreement with previous Pt_n studies.[55]

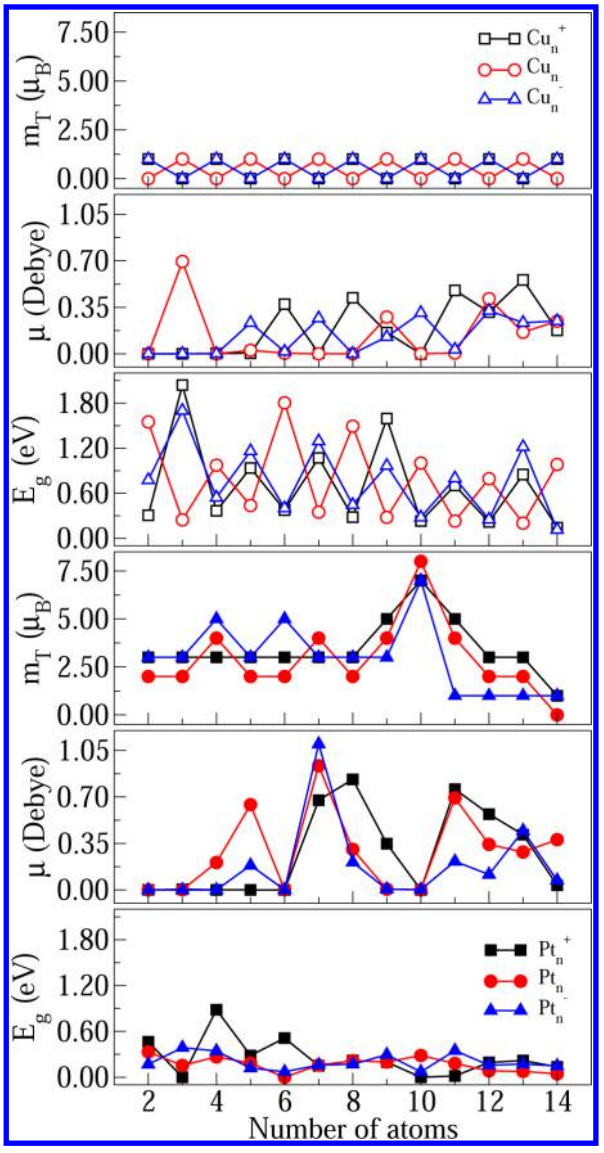

Figure 4. Total magnetic moment (m_T), dipole electric moment μ, and HOMO–LUMO energy gap E_g, of the Cu_n and Pt_n clusters in the lowest energy configurations (cationic, neutral, and anionic states) as a function of the number of atoms (n = 2–14).

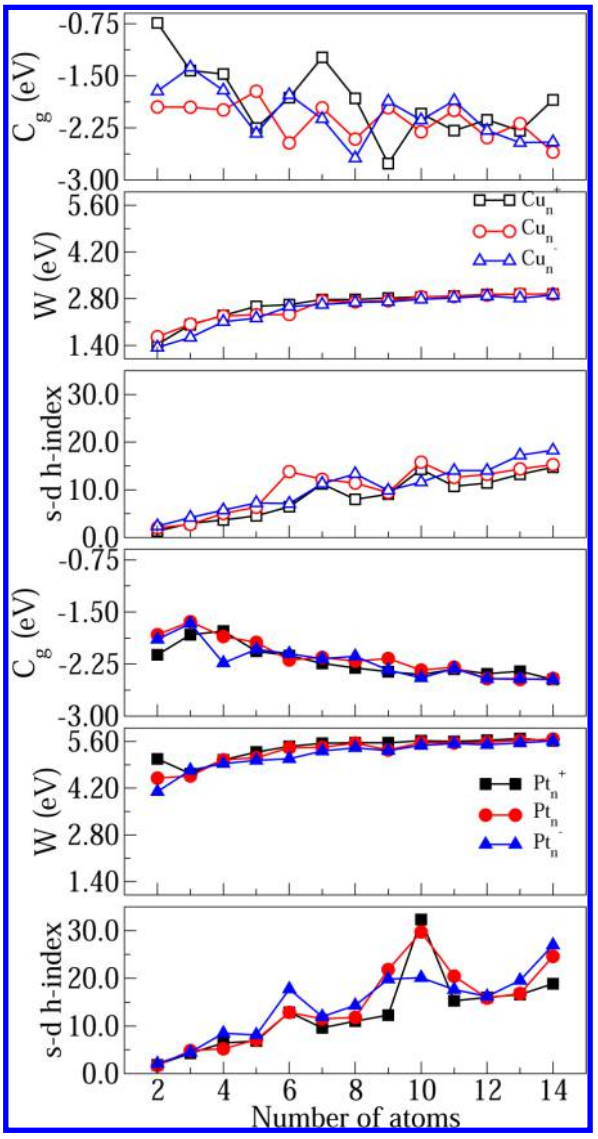

Figure 5. Center of gravity of the occupied d states (C_g), bandwidth of the occupied d states, W, and sd hybridization index for the Cu_n and Pt_n clusters in the lowest energy configurations (cationic, neutral, and anionic states) as a function of the number of atoms (n = 2–14).

Dipole Moment. Almost half of the Cu_n clusters have a zero dipole moment, while the remaining clusters have a value different from zero; for example, Cu_3^0 has the highest value (0.69 D). For Pt_n, the trends are also unclear; however, two

dx.doi.org/10.1021/jp508220h | J. Phys. Chem. A XXXX, XXX, XXX–XXX

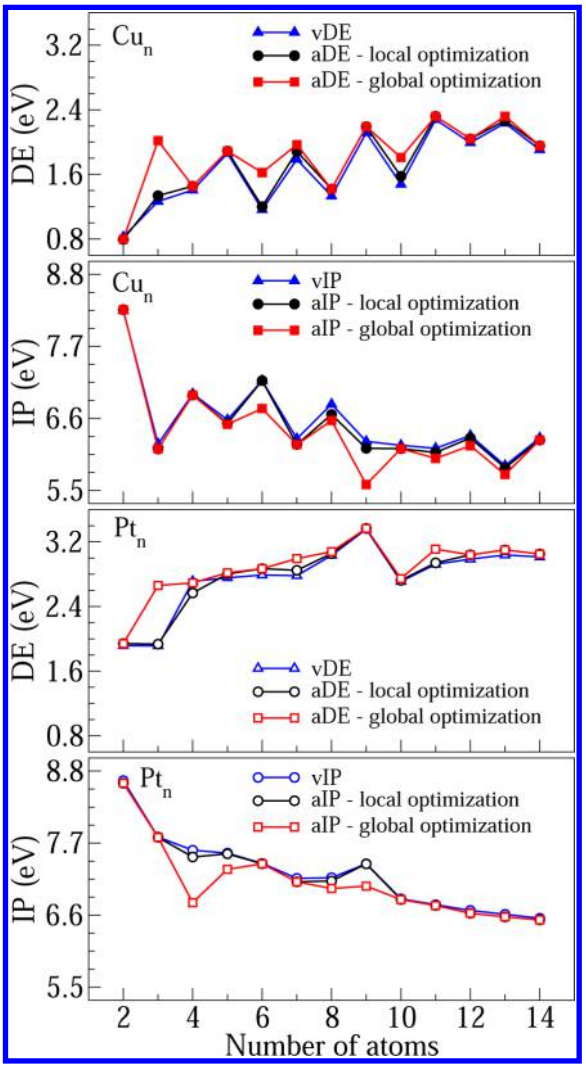

Figure 6. Detachment energy (DE) and ionization potential (IP) as a function of the number of atoms in the Cu_n and Pt_n clusters. vDE, vIP, aDE, and aIP are defined in Section II.

features emerge. Pt_7 has the highest dipole moment for all charge states, namely, 0.68 (+), 0.93 (0), and 1.10 D (−). In contrast, Pt_6 and Pt_{10} have almost zero dipole moment for all charge states, which are clusters that show high stability function values (ΔE^2) as well as high sd hybridization, which particularly enhances both the delocalization and the metallic character of the clusters. Furthermore, it can also be seen that Pt_7 has one of the lowest values for ΔE^2, which might indicate a correlation between dipole moment and stability.

HOMO−LUMO Energy Gap. For Pt_n^+, Pt_n^0, and Pt_n^-, the HOMO−LUMO gaps are from 0 to 0.4 eV, and, hence, even small Pt_n clusters start to show a metallic behavior. In contrast, Cu_n clusters show an oscillatory dependence on the even or odd number of electrons and highlight the possibility of tuning the energy gap values changing the cluster size and the charge state. For example, for Cu_n with an even number of electrons, we found E_g = 0.7−2.0 eV, which is reduced for odd number of electrons due to the unpaired electron, while an opposite behavior is observed for Cu_n^+ and Cu_n^-. Thus, these results indicate that small Cu clusters are far from a true metal system due to the large size of the HOMO−LUMO energy gaps. Those trends obtained for Pt_n and Cu_n can be explained in part by the location of the Fermi level in the Pt and Cu bulks, which cuts through the d band with a high density of states for Pt bulk and the sp band with a low density of states for Cu bulk. Furthermore, we did not find a relationship between the energy gaps and relative stability of the isomers, except for few cases, such as the magic cationic Pt clusters with n = 4 and 6 atoms, in which the HOMO lies in a region of low density of states.

Center of Gravity of the Occupied d States. The center of gravity of the occupied d states shows large oscillations, in particular, for the Cu_n clusters. Although the oscillations are present, the C_g results increase in absolute value, which indicates that the center of gravity of the occupied d states move away from the HOMO state. Thus, taking into account that the d band model[61,62] might be valid for clusters, which have been challenged by few cluster studies,[63] we would conclude that the reactivity depends on the cluster size, which is supported by experimental results.[13,59,64]

Bandwidth of the Occupied d States. Our cluster size effectively comprises the molecular limit, in which the density of states is discrete; in this sense, the term bandwidth used in this paper refers to the energy window where the discrete occupied d states lie. For both Cu_n and Pt_n clusters, the bandwidth of the occupied d states for the cationic, neutral, and anionic charge states increases for increased number of atoms in the clusters, which is expected as the broadening of the d states increases with an increased coordination number. Tiny oscillations can be noticed in the bandwidth, which can be attributed to the atomic structure of the clusters as there are 2D and 3D cluster configurations among the lowest energy configurations. Moreover, as anionic clusters tend to present smaller ECN values, their bandwidths tend to be slightly narrowed in comparison with neutral and cationic clusters.

Hybridization Index. For the lowest energy Pt_n clusters, peaks in the sd curves are located at Pt_6^+, Pt_{10}^+, Pt_6^-, Pt_9^-, Pt_{10}^-, Pt_{14}^-, Pt_6, Pt_{10}, and Pt_{14}. Therefore, we can notice a strong correlation between the sd hybridization and the stability function. Moreover, as pointed out in a previous study,[65] the Pt−Pt bond is affected by the delocalized s−s interactions, which is maximized by the sd hybridization with a negligible sp hybridization.

Detachment Energy and Ionization Potential. We obtained an even−odd alternation behavior for the DE and IP results for Cu_n clusters due to the electron-pairing effect. For example, it is more difficult to ionize even clusters than odd ones because even clusters have a closed-shell electronic structure. However, it is much easier to attach an electron to the odd clusters than the even ones. Although the oscillations are present, there is a clear increasing in the DE and decreasing in the IP. There is no similar oscillatory behavior for the Pt_n clusters due to the electronic structure; however, as observed for Cu_n, DE increases and IP decreases, except for few cases. For example, Pt_9 and Pt_{10} have large differences in the DE and IP, which is related to the great stability of the Pt_{10} cluster.

When only local optimization was employed to relax the structures, we found that vDE (vIP) and aDE (aIP) are very similar for both systems, with energy differences smaller than 0.17 eV. However, when we relaxed the structures using a *global optimization algorithm*, large differences between vDE (vIP) and aDE (aIP) were identified, in particular for the following systems: Cu_3, Cu_6 (DE), Cu_6, Cu_9 (IP), Pt_3 (DE), Pt_4, Pt_9 (IP). Those differences are related with the large changes in the atomic structures due to the increase or decrease in the number of electrons, which can be seen in Figure 1. Moreover, we assessed that $DE^{Pt_n} > DE^{Cu_n}$, and, hence, it is easier to attach

dx.doi.org/10.1021/jp508220h | J. Phys. Chem. A XXXX, XXX, XXX−XXX

one electron to the Pt_n clusters than to the Cu_n ones. A similar trend is obtained for IP, $IP^{Pt_n} > IP^{Cu_n}$, and, hence, it is easier to remove one electron from Cu_n clusters, except for Cu_4. In general, our DE and IP results with *global optimization* largely improve the agreement with previous results[48,58,66−69] in comparison with our DE and IP results obtained with local optimizations.

IV. DISCUSSION

According to our results summarized above and in the Supporting Information, the properties are in general very susceptible to the charge state. For example, a single electron can strongly alter the geometry of a cluster, an effect that must be taken into account in a thorough theoretical study; otherwise, comparisons between simulations and experiments become impaired. In particular, we found a clear tendency showing that increasing electron density triggers geometrical alterations associated with decreasing the ECN for both Cu_n and Pt_n clusters, which is in line with the results obtained for Au_7 clusters in the gas phase using vibrational spectroscopy, where the addition of one electron favors more open structures.[8] In contrast, cationic clusters with one less electron tend to present more compact structures, that is, present higher number of neighboring atoms increasing ECN values, which induces the planar-to-3D transition to occur earlier for these systems. These charge effects cause a ubiquitous decrease in the *bandwidth* of the occupied d states for anionic clusters in comparison with neutral and cationic ones. Additionally, Pt clusters tend to be less compact than Cu ones, which is due to the less localized nature of the d states and stronger sd hybridization in Pt_n clusters, which affects the binding mechanism for small clusters. Thus, it increases the directional character of the Pt−Pt bond and, hence, favors more open structures.

Our analysis for energetic properties shows that the E_b curve for the anions lies between those of the neutrals and the cations, indicating that the last ones present higher binding energies. In general, these curves increase almost monotonically with size for all charge states, being disrupted at certain magic number sizes. For Cu_n clusters we observed the characteristic odd−even alternation due to the electron-pairing effect, while for Pt_n clusters, humps in the E_b curves occur for particular Pt_n clusters, which indicates higher relative stability of those clusters consistent with the stability function results. Remarkably, Pt_6 and Pt_{10} present very high stability for all charge states, and similar structures are observed for both charge states, namely, a 2D structure composed by interconnected triangles for Pt_6 and a pyramidal structure composed by Pt_6 motifs for Pt_{10}. Our results indicate that the sd hybridization is one of the main mechanisms for the Pt_n cluster stabilization. We found that the high sd hybridization index for Pt_{10}, Pt_{10}^-, and Pt_{10}^+ does not lead to a decrease in the magnetic moment; rather, these clusters present the highest magnetic moments, in contrast to Ni clusters, for which the onset of significant sd hybridization, ∼10 Ni atoms, is responsible for the reduction of the magnetic moments.[70] Given the highly symmetric structure of Pt_{10}, the enhancement in the spin magnetic moment is attributed to the favored exchange coupling over a possible competing Jahn−Teller distortion.

The electron pairing is a well-known effect for Cu clusters,[45] which is also present for our case, where the even−odd oscillation is ubiquitous, influencing the HOMO−LUMO gap, the magnetic moment, the detachment energy, the ionization potential, the center of gravity of the occupied d states, and the stability function. However, the behavior of electric dipole moment and sd hybridization index does not present this clear even−odd alternation trend and does not have a straightforward answer. In turn, for Pt clusters an attempt is proposed to correlate electric dipole moment with stability. High sd hybridization index, very related with the stabilization of Pt clusters, particularly enhances both electronic delocalization and metallic character decreasing the electric dipole of these systems. For example, we found that for the very stable Pt_6 and Pt_{10} clusters the electric dipole moments are almost zero for all cluster charges. Furthermore, the center of gravity of the occupied d states shows large oscillations, and in general, it moves away from the HOMO state highlighting the dependence of the reactivity with the number of atoms and with the charge state as well. Pt_n clusters present smaller HOMO−LUMO gaps than Cu_n clusters mainly due to the greater density of states at the Fermi energy for Pt_n clusters.[65] Further, our results do not suggest any correlation between high cluster magnetic moments and large HOMO−LUMO gaps, as indicated earlier by Xiao et al.[51]

V. CONCLUSIONS

In this paper we addressed the study of Cu_n and Pt_n clusters for $n = 2−14$ in the cationic, neutral, and anionic states. Our cluster geometries were determined via symmetry-unrestricted structural optimizations through an extensive search among various structures for each size and state of charge. Although this approach is very computationally demanding, it enabled a more realistic description of our systems allowing us to obtain energy orderings for each size and state of charge as well. Thus, we also considered (Supporting Information) high-energy isomers and not only the properties from the lowest energy structures, which permits a well-established comparison with experimental results.

The most important conclusions are (i) the properties are in general very susceptible to the charge state; in particular, the structures tend to decrease the atomic coordination when one electron is added to the system, which strongly affects the transition from 2D to 3D configurations. (ii) The Pt_6 and Pt_{10} clusters present very high stability for all charge states, which can be clearly correlated with high sd hybridization and null electric dipole moments. (iii) In turn, Pt_{10} clusters present the highest magnetic moments for all charge states. (iv) For Cu_n clusters, the HOMO−LUMO gap, the magnetic moment, the detachment energy, the ionization potential, the center of gravity of the occupied d states, and the stability function show the even−odd oscillation behavior due to the electron-pairing effect. However, the behavior of electric dipole moment and sd hybridization index does not present this clear even−odd alternation trend. (v) In general, Pt clusters are less compact than Cu ones, which is due to the less localized nature of the d states and stronger sd hybridization in Pt_n clusters.

■ ASSOCIATED CONTENT

Supporting Information

The analyses for the high-energy isomers are reported. This material is available free of charge via the Internet at http://pubs.acs.org.

■ AUTHOR INFORMATION

Corresponding Authors

*E-mail: ascbonelli@gmail.com (A.S.C.).

*E-mail: rondina@gmail.com (G.G.R.).
*E-mail: mauriciomjp@gmail.com (M.J.P.).
*E-mail: pltereshchuk@mail.ru (P.T.).
*E-mail: juarez_dasilva@iqsc.usp.br Phone: +55 16 3373 6641. Fax: +55 16 3373 9952. (J.L.F.D.S.).

Notes

The authors declare no competing financial interest.

■ ACKNOWLEDGMENTS

The authors thank the São Paulo Research Foundation (FAPESP), National Council for Scientific and Technological Development (CNPq), Coordination for Improvement of Higher Level Education (CAPES), and Rio Grande do Sul State Research Foundation (FAPERGS) for the financial support. The authors thank also Laboratory of Advanced Scientific Computing for the computing time and the Department of Information Technology, Campus São Carlos, for the infrastructure provided to our computer cluster.

■ ABBREVIATIONS

DFT; PBE; KS; NAOs; FHI-aims

■ REFERENCES

(1) Baletto, F.; Ferrando, R. Structural properties of nanoclusters: Energetic, thermodynamic, and kinetic effects. *Rev. Mod. Phys.* **2005**, *77*, 371−423.
(2) Castleman, A. W., Jr.; Khanna, S. N. Clusters, Superatoms, and Building Blocks of New Materials. *J. Phys. Chem. C* **2009**, *113*, 2664−2675.
(3) Cândido, L.; Rabelo, J. N. T.; Da Silva, J. L. F.; Hai, G.-Q. Quantum Monte Carlo Study of Small Aluminum Clusters Al_n (n = 213). *Phys. Rev. B* **2012**, *85*, 245404.
(4) Da Silva, J. L. F.; Piotrowski, M. J.; Aguilera-Granja, F. Hybrid Density Functional Study of Small Rh_n (n = 2 − 15) Clusters. *Phys. Rev. B* **2012**, *86*, 125430.
(5) Piotrowski, M. J.; Piquini, P.; Da Silva, J. L. F. Density Functional Theory Investigation of 3*d*, 4*d*, and 5*d* 13-atom Metal Clusters. *Phys. Rev. B* **2010**, *81*, 155446.
(6) Fielicke, A.; Kirilyuk, A.; Ratsch, C.; Behler, J.; Scheffler, M.; von Helden, G.; Meijer, G. Structure Determination of Isolated Metal Clusters via Far-Infrared Spectroscopy. *Phys. Rev. Lett.* **2004**, *93*, 023401.
(7) Weis, P. Structure Determination of Gaseous Metal and Semimetal Cluster Ions by Ion Mobility Spectrometry. *Int. J. Mass Spectrom.* **2005**, *245*, 1−13.
(8) Gruene, P.; Rayner, D. M.; Redlich, B.; van der Meer, A. F. G.; Lyon, J. T.; Meijer, G.; Fielicke, A. Structures of neutral Au_7, Au_19, and Au_20 clusters in the gas phase. *Science* **2008**, *321*, 674.
(9) Shayeghi, A.; Johnston, R. L.; Schäfer, R. Evaluation of Photodissociation Spectroscopy as a Structure Elucidation Tool for Isolated Clusters: A Case Study of Ag_4^+ and Au_4^+. *Phys. Chem. Chem. Phys.* **2013**, *15*, 19715.
(10) Berg, C.; Beyer, M.; Achatz, U.; Joos, S.; Niedner-Schatteburg, G.; Bondybeya, V. E. Effect of charge upon metal cluster chemistry: Reactions of Nb_n and Rh_n anions and cations with benzene. *J. Chem. Phys.* **1998**, *108*, 5398−5403.
(11) Achatz, U.; Berg, C.; Joos, S.; Fox, B. S.; Beyer, M. K.; Niedner-Schatteburg, G.; Bondybey, V. E. Methane Activation by Platinum Cluster Ions in the Gas Phase: Effects of Cluster Charge on the Pt_4 tetramer. *Chem. Phys. Lett.* **2000**, *320*, 53−58.
(12) Yoon, B.; Häkkinen, H.; Landman, U.; Wörz, A. S.; Antonietti, J.-M.; Abbet, S.; Judai, K.; Heiz, U. Charging Effects on Bonding and Catalyzed Oxidation of CO on Au_8 Clusters on MgO. *Science* **2005**, *307*, 403.
(13) Adlhart, C.; Uggerud, E. Reactions of Platinum Clusters $Pt_n^{\pm}$, n = 1 − 21, with CH_4: To React or Not To React. *Chem. Commun.* **2006**, 2581−2582.
(14) Harding, D.; Kerpal, C.; Rayner, D. M.; Fielicke, A. Communication: The Structures of Small Cationic Gas-Phase Platinum Clusters. *J. Chem. Phys.* **2012**, *136*, 211103.
(15) Wales, D. J.; Doye, J. P. K. Global optimization by basin-hopping and the lowest energy structures of Lennard-Jones clusters containing up to 110 atoms. *J. Phys. Chem. A* **1997**, *101*, 5111−5116.
(16) Doye, J. P. K.; Wales, D. J. Global Minima for Transition Metal Clusters Described by Sutton-Chen Potentials. *New. J. Chem.* **1998**, *22*, 733.
(17) Rondina, G. G.; Da Silva, J. L. F. A Revised Basin-Hopping Monte Carlo Algorithm for Structure Optimization of Clusters and Nanoparticles. *J. Chem. Inf. Model.* **2013**, *53*, 2282−2298.
(18) Johnston, R. L. Evolving better nanoparticles: Genetic algorithms for optimizing cluster geometries. *Dalton Trans.* **2003**, 4193−4207.
(19) Lai, X.; Huang, W.; Xu, R. Geometry Optimization of Atomic Clusters Using a Heuristic Method with Dynamic Lattice Searching. *J. Phys. Chem. A* **2011**, *115*, 5021−5026.
(20) Piotrowski, M. J.; Piquini, P.; Odashima, M. M.; Da Silva, J. L. F. Transition-Metal 13-Atom Clusters Assessed with Solid and Surface-Biased Functionals. *J. Chem. Phys.* **2011**, *134*, 134105.
(21) Doye, J. P. K.; Wales, D. J. Saddle Points and Dynamics of Lennard-Jones Clusters, Solids, and Supercooled Liquids. *J. Chem. Phys.* **2002**, *116*, 3777.
(22) Wales, D. J.; Doye, J. P. K. Stationary Points and Dynamics in High-Dimensional Systems. *J. Chem. Phys.* **2003**, *119*, 12409.
(23) Wu, M.; Kandalam, A. K.; Gutsev, G. L.; Jena, P. Origin of the Anomalous Magnetic Behavior of the Fe_{13}^+ Cluster. *Phys. Rev. B* **2012**, *86*, 174410.
(24) Gutsev, G. L.; Weatherford, C. W.; Belay, K. G.; Ramachandran, B. R.; Jena, P. An All-Electron Density Functional Theory Study of the Structure and Properties of the Neutral and Singly Charged M_{12} and M_{13} Clusters: M = Sc-Zn. *J. Chem. Phys.* **2013**, *138*, 164303.
(25) Gilb, S.; Weis, P.; Furche, F.; Ahlrichs, R.; Kappes, M. M. Structures of Small Gold Cluster Cations (Au_n^+, n < 14): Ion Mobility Measurements versus Density Functional Calculations. *J. Chem. Phys.* **2002**, *116*, 4094−4101.
(26) Furche, F.; Ahlrichs, R.; Weis, P.; Jacob, C.; Gilb, S. The structures of small gold cluster anions as determined by a combination of ion mobility measurements and density functional calculations. *J. Chem. Phys.* **2002**, *117*, 6982−6990.
(27) Taylor, S.; Lemire, G. W.; Hamrick, Y. M.; Fu, Z.; Morse, M. D. Resonant Two-Photon Ionization Spectroscopy of Jet-Cooled Pt_2. *J. Chem. Phys.* **1988**, *89*, 5517−5523.
(28) Eberhardt, W.; Fayet, P.; Cox, D. M.; Fu, Z.; Kaldor, A.; Sherwood, R.; Sondericker, D. Photoemission from Mass-Selected Monodispersed Pt Clusters. *Phys. Rev. Lett.* **1990**, *64*, 780−783.
(29) Ho, J.; Polak, M. L.; Ervin, K. M.; Lineberger, W. C. Photoelectron Spectroscopy of Nickel Group Dimers: Ni_2^-, Pd_2^-, and Pt_2^-. *J. Chem. Phys.* **1993**, *99*, 8542.
(30) Celep, G.; Cottancin, E.; Lermé, J.; Pellarin, M.; Arnaud, L.; Huntzinger, J. R.; Vialle, J. L.; Broyer, M.; Palpant, B.; Boisron, O.; et al. Optical Properties of Copper Clusters Embedded in Alumina: An Experimental and Theoretical study of Size Dependence. *Phys. Rev. B* **2004**, *70*, 165409.
(31) Lecoultre, S.; Rydlo, A.; Félix, C.; Buttet, J.; Gilb, S.; Harbich, W. Optical Absorption of Small Copper Clusters in Neon: Cu_n, (n = 1 − 9). *J. Chem. Phys.* **2011**, *134*, 074303.
(32) Heredia, C. L.; Ferraresi-Curotto, V.; López, M. B. Characterization of Pt_n (n = 2−12) Clusters through Global Reactivity Descriptors and Vibrational Spectroscopy, a Theoretical Study. *Comput. Mater. Sci.* **2012**, *53*, 18−24.
(33) Perdew, J. P.; Chevary, J. A.; Vosko, S. H.; Jackson, K. A.; Pederson, M. R.; Singh, D. J.; Fiolhais, C. Atoms, Molecules, Solids, and Surfaces: Applications of the Generalized Gradient Approximation

for Exchange and Correlation PW91 Reference. *Phys. Rev. B* **1992**, *46*, 6671−6687.
(34) Perdew, J. P.; Burke, K.; Ernzerhof, M. Generalized Gradient Approximation Made Simple. *Phys. Rev. Lett.* **1996**, *77*, 3865−3868.
(35) Blum, V.; Gehrke, R.; Hanke, F.; Havu, P.; Havu, V.; Ren, X.; Reuter, K.; Scheffler, M. Ab Initio Molecular Simulations with Numeric Atom-Centered Orbitals. *Comput. Phys. Commun.* **2009**, *180*, 2175−2196.
(36) Havu, V.; Blum, V.; Havu, P.; Scheffler, M. Efficient O(N) integration for all-electron electronic structure calculation using numeric basis functions. *Comput. Phys. Commun.* **2009**, *228*, 8367−8379.
(37) van Lenthe, E.; Snijders, J. G.; Baerends, E. J. The zero-order regular approximation for relativistic effects: The effect of spin-orbit coupling in closed shell molecules. *J. Chem. Phys.* **1996**, *105*, 6505−6516.
(38) Averill, F. W.; Ellis, D. E. An Efficient Numerical Multicenter Basis Set for Molecular Orbital Calculations: Application to $FeCl_4$. *J. Chem. Phys.* **1973**, *59*, 6412−6418.
(39) Zunger, A.; Freeman, A. J. Self-Consistent Numerical-Basis-Set Linear-Combination-of-Atomic-Orbitals Model for the Study of Solids in the Local Density Formalism. *Phys. Rev. B* **1977**, *15*, 4716−4737.
(40) Sutton, A. P.; Chen, J. *Philos. Mag. Lett.* **1990**, *61*, 139.
(41) Hanwell, M. D.; Curtis, D. E.; Lonie, D. C.; Vandermeersch, T.; Zurek, E.; Hutchison, G. R. Avogadro: An Advanced Semantic Chemical Editor, Visualization, and Analysis Platform. *J. Cheminf.* **2012**, *4*, 17.
(42) Hoppe, R. Effective Coordination Numbers (ECoN) and Mean Fictive Ionic Radii (MEFIR). *Z. Kristallogr.* **1979**, *150*, 23−52.
(43) Da Silva, J. L. F.; Kim, H. G.; Piotrowski, M. J.; Prieto, M. J.; Tremiliosi-Filho, G. Reconstruction of Core and Surface Nanoparticles: The Example of Pt_{55} and Au_{55}. *Phys. Rev. B* **2010**, *82*, 205424.
(44) Da Silva, J. L. F. Effective Coordination Concept Applied for Phase Change $(GeTe)_m(Sb_2Te_3)_n$ Compounds. *J. Appl. Phys.* **2011**, *109*, 023502.
(45) Chu, X.; Xiang, M.; Zeng, Q.; Zhu, W.; Yang, M. Competition Between Monomer and Dimer Fragmentation Pathways of Cationic Cu_n Clusters of $n = 2 - 20$. *J. Phys. B: At., Mol. Opt. Phys.* **2011**, *44*, 205103.
(46) Molayem, M.; Grigoryan, V. G.; Springborg, M. Theoretical Determination of the Most Stable Structures of Ni_mAg_n Bimetallic Nanoalloys. *J. Phys. Chem. C* **2011**, *115*, 7179−7192.
(47) Häkkinen, H.; Moseler, M.; Landman, U. Bonding in Cu, Ag, and Au Clusters: Relativistic Effects, Trends, and Surprises. *Phys. Rev. Lett.* **2002**, *89*, 033401.
(48) Yang, M.; Jackson, K. A.; Koehler, C.; Frauenheim, T.; Jellinek, J. Structure and shape variations in intermediate-size copper clusters. *J. Chem. Phys.* **2006**, *124*, 024308.
(49) Guvelioglu, G. H.; Ma, P.; He, X.; Forrey, R. C.; Cheng, H. Evolution of Small Copper Clusters and Dissociative Chemisorption of Hydrogen. *Phys. Rev. Lett.* **2005**, *94*, 026103.
(50) Sebetci, A.; Güvenc, Z. B. Energetics and Structures of Small Clusters: Pt_n, $n = 2 - 21$. *Surf. Sci.* **2003**, *525*, 66−84.
(51) Xiao, L.; Wang, L. Structures of Platinum clusters: planar or spherical. *J. Phys. Chem. A* **2004**, *108*, 8605−8614.
(52) Futschek, T.; Hafner, J.; Marsman, M. Stable structural and magnetic isomers of small transition-metal clusters from the Ni group: an *ab initio* density-functional study. *J. Phys.: Condens. Matter* **2006**, *18*, 9703−9748.
(53) Bhattacharyya, K.; Majumder, C. Growth pattern and bonding trends in Pt_n ($n = 2 - 13$) clusters: Theoretical investigation based on first principle calculations. *Chem. Phys. Lett.* **2007**, *446*, 374.
(54) Nie, A.; Wu, J.; Zhou, C.; Yao, S.; Luo, C.; Forrey, R. C.; Cheng, H. Structural Evolution of Subnano Platinum Clusters. *Int. J. Quantum Chem.* **2007**, *107*, 219−224.
(55) Kumar, V.; Kawazoe, Y. Evolution of Atomic and Electronic Structure of Pt Clusters: Planar, Layered, Pyramidal, Cage, Cubic, and Octahedral Growth. *Phys. Rev. B* **2008**, *77*, 205418.
(56) Fortunelli, A. Density Functional Calculations on Small Platinum Clusters: Pt_n^q ($n = 1 - 4$, $q = 0 \pm 1$). *J. Mol. Struct.: THEOCHEM* **1999**, *493*, 233−240.
(57) Kittel, C. *Introduction to Solid State Physics*, 7th ed.; John Wiley & Sons: New York, 1996.
(58) Jug, K.; Zimmermann, B.; Calaminici, P.; Koster, A. M. Structure and stability of small copper clusters. *J. Chem. Phys.* **2002**, *116*, 4497.
(59) Hirabayashi, S.; Ichihashi, M.; Kawazoe, Y.; Kondow, T. Comparison of Adsorption Probabilities of O_2 and CO on Copper Cluster Cations and Anions. *J. Phys. Chem. A* **2012**, *116*, 8799−8806.
(60) Luo, W.; Pennycook, S. J.; Pantelides, S. T. s-Electron Ferromagnetism in Gold and Silver Nanoclusters. *Nano Lett.* **2007**, *7*, 3134−3137.
(61) Hammer, B.; Nørskov, J. K. *Advances in Catalysis;* Academic Press, Inc.: San Diego, 2000.
(62) Kitchin, J. R.; Nørskov, J. K.; Barteau, M. A.; Chen, J. G. Role of Strain and Ligand Effects in the Modification of the Electronic and Chemical Properties of Bimetallic Surfaces. *Phys. Rev. Lett.* **2004**, *93*, 156801.
(63) Piotrowski, M. J.; Piquini, P.; Zeng, Z.; Da Silva, J. L. F. Adsorption of NO on the Rh_{13}, Pd_{13}, Ir_{13}, and Pt_{13} Clusters: A Density Functional Theory Investigation. *J. Phys. Chem. C* **2012**, *116*, 20540.
(64) Knickelbein, M. B. Reactions of Transition Metal Clusters with Small Molecules. *Annu. Rev. Phys. Chem.* **1999**, *50*, 79−115.
(65) Wang, H.; Carter, E. A. Metal-Metal Bonding in Transition-Metal Clusters with Open d Shells: Pt_3. *J. Phys. Chem.* **1992**, *96*, 1197−1204.
(66) Gronbeck, H.; Andreoni, W. Gold and platinum microclusters and their anions: comparison of structural and electronic properties. *Chem. Phys.* **2000**, *262*, 1−14.
(67) Pettiette, C. L.; Yang, S. H.; Craycraft, M. J.; Conceicao, J.; Laaksonen, R. T.; Cheshnovsky, O.; Smalley, R. E. Ultraviolet Photoelectron Spectroscopy of Copper Clusters. *J. Chem. Phys.* **1988**, *88*, 5377.
(68) Knickelbein, M. B. Electronic Shell Structure in the Ionization of Copper Clusters. *Chem. Phys. Lett.* **1992**, *192*, 129−134.
(69) Ganteför, G.; Eberhardt, W. Localization of 3*d* and 4*d* Electrons in Small Clusters: The Roots of Magnetism. *Phys. Rev. Lett.* **1996**, *76*, 4975−4978.
(70) Liu, S.-R.; Zhai, H.-J.; Wang, L.-S. $s - d$ hybridization and evolution of the electronic and magnetic properties in small Co and Ni clusters. *Phys. Rev. B* **2002**, *65*, 113401.